Temperature dependence of plasmons in Nb-doped $SrTiO_3$

François Gervais and Jean-Louis Servoin
Centre de Recherches sur la Physique des Hautes Températures, Centre National de la Recherche Scientifique, 45071 Orléans CEDEX 2, France

Alexis Baratoff, Johannes G. Bednorz, and Gerd Binnig
IBM Zürich Research Laboratory, 8803 Rüschlikon, Switzerland
(Received 17 August 1992; revised manuscript received 8 December 1992)

The temperature dependence of infrared reflection spectra of single crystals of *n*-type strontium titanate doped with 0.3 to 1.5 at. % niobium are reported from 10 to 5 000 cm^{-1} in the temperature range 80–900 K. Results are analyzed by means of various factorized forms of the dielectric function. A decoupling scheme allows the temperature dependence of the plasmon to be deduced. The plasma frequency of the carriers is found to *increase* upon cooling, a very unusual phenomenon which, together with Hall-effect measurements, may imply that the effective mass of the carriers decreases upon cooling. The dependence of the soft ferroelectric mode on temperature and Nb doping is also reported and discussed.

I. INTRODUCTION

The discovery of high-temperature superconductivity in lanthanum barium copper oxide by Bednorz and Müller[1] raises an important problem of understanding which is not yet solved even after 6 years of extensive investigations. A large part of the difficulties comes from our poor understanding of conducting properties of oxides in the normal state above T_c. Optical properties are very unusual, in particular in the infrared with a response of charge carriers which seems to deviate from a simple Drude profile (see, e.g., the review paper by Timusk and Tanner[2]). Strontium titanate doped with niobium, or reduced under hydrogen at high temperature, becomes an *n*-type conductor with an electronic concentration ranging from 10^{19} to 3×10^{20} cm^{-3}. It has been known for nearly 30 years to become superconducting below a temperature which, however, does not exceed 0.7 K.[3,4] There is no bidimensionality in this case which is a simple-cubic perovskite structure, and no itinerant Jahn-Teller phenomena, as in copper compounds. The only other examples of superconducting oxides with the perovskite structure and no magnetic ion are bismuth compounds $Ba(Pb,Bi)O_3$ and $(Ba,K)BiO_3$.[5,6] This last family is particularly interesting in that superconductivity has also been recently discovered in the two-dimensional (2D) parent $(Ba,K)_2(Pb,Bi)O_4$ which crystallizes in the tetragonal K_2NiF_4-type structure, as $(La,Sr)_2CuO_4$.[7] T_c is found higher than in the 3D case with the same bismuth rate, although the electronic concentration does not exceed 2×10^{20} cm^{-3} whereas it is much higher in the 3D compounds.[8] This is the only example that we are aware of with superconductivity in both 2D and 3D structures built with the same ions.

The chemical bonding in transition-metal oxides is particularly interesting in that it is partially ionic, partially covalent, and also possibly metallic in those cases where the polarizability is enhanced, giving rise to complete delocalization of the electrons of the outer shell. As a result, they may exhibit very different properties depending on small changes of bonding with temperature, pressure, or doping. Certain oxides with the rutile structure like NbO_2 or VO_2 thus undergo an insulator-metal phase transition, whereas compounds like SnO_2 or GeO_2, that are very similar crystallographically, remain insulating at any temperature or pressure.[9] The hybridization of oxygen *p* states with the transition-metal *d* states has been shown to be at the origin of ferroelectricity in oxide perovskites like barium titanate or potassium niobate.[10–14]

Within this framework, strontium titanate is a good candidate for further investigations. (i) First because, under ceramic form, this is a material for technological applications as a capacitor. (ii) In addition, upon reduction[15,16] or doping,[17] strontium titanate becomes an *n*-type conductor as mentioned above, thus also being interesting in the field of electronic ceramics. A plasmon mode is expected at sufficiently high carrier concentration. However, the observation of the plasmon by infrared reflectivity is not straightforward in highly polar crystals like TiO_2 rutile[18] or oxidic perovskites because contributions from most polar phonons which are present in those compounds, in relation with their ferroelectric (FE) or incipient FE properties, can mask that of the plasmon when its frequency lies within the same spectral domain. Plasma waves are longitudinal excitations which couple to longitudinal-optical (LO) phonons. A large shift of the highest-frequency LO mode with temperature or defect concentration is a conspicuous experimental signature of a coupled LO phonon-plasmon system. (iii) The study of the electron-phonon coupling mechanisms in *n*-type $SrTiO_3$ is especially interesting because such semiconductors become superconducting below 0.7 K for a carrier concentration which does not exceed 10^{20} cm^{-3}.

II. INFRARED REFLECTIVITY

A. Experiment

Strontium titanate single crystals doped with 0.6, 0.9, and 1.5 at. % of niobium have been investigated by infrared reflectivity spectroscopy in the temperature range from 80 to 900 K. The Fourier spectrometer BRUKER IFS 113 we have used covers the wave-number range from 10 to 5000 cm^{-1}. The spectrometer and the device for measurements up to high temperature have been described elsewhere.[19]

Approximately 6×11 mm^2 [001] crystal faces were optically polished and exhibited a reflectivity in the near infrared, around 2 μm, quite comparable to those found in undoped strontium titanate. However, the spectra are significantly modified in the regions showing minimum negative slope, roughly corresponding to LO frequencies. The penetration depth of infrared radiation in doped samples is relatively small since the absorption coefficient ranges from 5000 cm^{-1} in the near infrared (penetration depth 2 μm) to 28 000 cm^{-1} (penetration depth 0.35 μm) near the ferroelectric soft-mode frequency in the sample doped with 0.9% Nb, for example. Samples, therefore, must be annealed at high temperatures to regenerate the surface partially altered by polishing, in order to reflect bulk properties. Figure 1 shows the effect of an annealing temperature on the room-temperature spectrum of the sample doped with 0.6% Nb. No such effect is observed in undoped crystals. If we anticipate on the analysis of the spectra, annealing at 900 K decreases the plasmon damping parameter by a factor of 3 while the plasma frequency remains unaffected. Annealing also has little effect on phonon frequencies but reduces phonon linewidths as well. The decrease of linewidths is the signature of reordering. It is known indeed that the spectra of disordered systems such as glasses show broad bands. Since the plasmon dominates the reflectivity, the variation of plasmon damping related to reordering is the cause of major modification of the spectral profiles. The spectra analyzed in the next section were recorded after annealing at 1000 K for 2 h in air, followed by slow cooling. This thermal treatment is thus found to relax the local constraints due to crystal growth and reorder the system.

B. Data analysis

Typical infrared reflection spectra obtained at various temperatures and in two different samples are displayed in Figs. 2 and 3. As indicated already by Spitzer *et al.*,[20] no choice of damping rate γ_{TO} of the soft FE mode in compounds like rutile or oxidic perovskites yields a satisfactory fit to reflectivity data in the infrared if the classical dispersion formula

$$\varepsilon=\varepsilon_\infty+\sum_j \Delta\varepsilon_j\Omega_{jTO}^2/(\Omega_{jTO}^2-\omega^2+i\gamma_{jTO}\omega) \quad (1)$$

is used. This is because, in those compounds, the soft mode dominates the reflectivity in the spectral range 10–1000 cm^{-1} owing to its unusually high oscillator strength $\Delta\varepsilon$. For that reason, Barker and Hopfield introduced a mode-coupling formalism[21] to fit the reflectivity spectra of such crystals. Later, Ledsham, Chambers, and Parker[22] pointed out that the resulting damping for the decoupled high-frequency mode is always negative, just as in their own analysis of potassium dihydrogen phosphate (KDP) where the same mode-coupling formalism was used. They concluded, therefore, that this model is a curve-fitting procedure without much physical content. Gervais and Baumard[23] subsequently proposed an alternative model to solve the problem not only in pure, but also in reduced rutile. The model was shown to yield better fitting in oxidic perovskites too.[12,13,19] This model introduces a fourth adjustable parameter for each TO-LO pair, viz., the damping parameter γ_{jLO} of the jth LO mode, which may be different from that, γ_{jTO}, of the associated TO mode. Note that Eq. (1) implicitly assumes $\gamma_{TO}=\gamma_{LO}$ in the case of a single mode.[19] The resulting improvement is particularly significant when the TO-LO splitting is large, as in the materials in question, because the TO and LO modes then have quite different phonon decay channels and, therefore, very different damping rates. In the model in question, the dielectric function is simply written as a product over pairs of complex poles and zeros believed to be relevant in the frequency range covered by the measurements,

$$\varepsilon=\varepsilon_\infty\prod_j(\Omega_{jLO}^2-\omega^2+i\gamma_{jLO}\omega)/(\Omega_{jTO}^2-\omega^2+i\gamma_{jTO}\omega)\ . \quad (2)$$

This model represents a powerful alternative to the

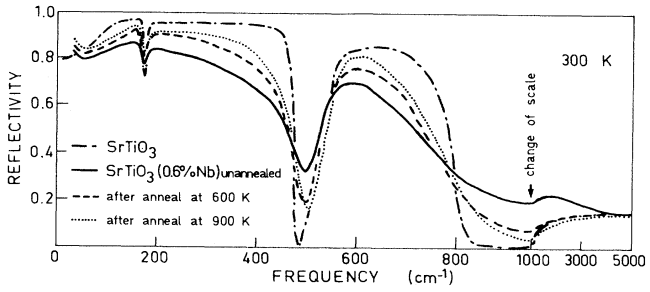

FIG. 1. Dependence of an infrared reflection spectrum of a polished sample on temperature of annealing in air. In this figure and the subsequent ones, percentages are atoms percent.

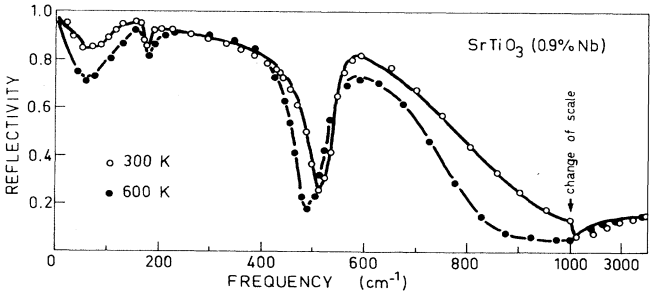

FIG. 2. Infrared reflection spectrum of preannealed sample at two temperatures. Symbols represent experimental data and solid curves are the best fit of the factorized form of the dielectric function equation (2) to the data.

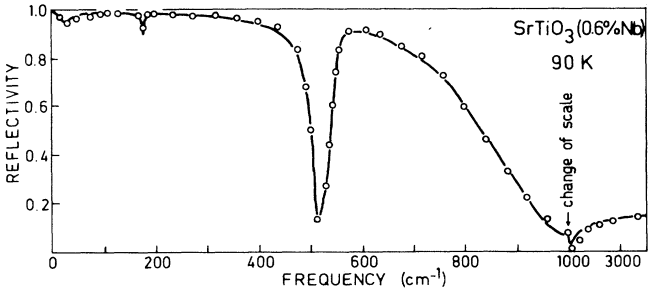

FIG. 3. Same as Fig. 2 for another sample.

Kramers-Kronig (KK) analysis which is commonly used, and is unbiased in principle, but in practice requires assumptions about the dependence of the dielectric response outside the range of measurement. The dispersion of the plasmon extends down to zero frequency, which just raises a specific problem with KK analysis. Note that the Ω_j's are the moduli of the complex poles (or zeros) of the dielectric function and not their real part. Equation (2) is also valid for a plasmon-phonon-coupled system[18,19] provided one of the TO frequencies is set equal to zero. With this constraint, a fit of Eq. (2) to experimental reflectivity for the sample doped with 0.9% Nb is shown in Fig. 2 at two temperatures and found to closely reproduce the spectra in the whole range 20–5000 cm^{-1}. This is especially significant since spectra of *n*-type $SrTiO_3$ reported in the literature were incomplete in the far infrared (no data below 350 cm^{-1} in Ref. 15 and below 400 cm^{-1} in Ref. 17). The parameters which yield the best fit to reflectivity data at room temperature and 600 K are listed in Table I. The results indicate that TO phonons are little affected by doping compared with parameters found in undoped $SrTiO_3$ with the same method[12] which are also listed in Table I. There is one exception, however, the TO soft FE mode which will be discussed in a specific paragraph. The high-frequency dielectric constant ε_∞ is not significantly modified by doping either. This is true for all samples and at all temperatures investigated. On the other hand, a new nearly overdamped LO mode appears below the TO soft FE mode. The highest-frequency LO mode exhibits a shift from 924 cm^{-1} at 300 K down to 817 cm^{-1} at 600 K, and an unusually strong damping increase, up to several hundred cm^{-1}. Both effects are large and clearly unrelated to the physics of LO phonons in undoped $SrTiO_3$ which has already been investigated in this temperature range.[12] This point deserves emphasis because (i) these phenomena can be safely assigned to plasmon-phonon coupling signature, and (ii) the shift of the highest LO mode observed upon heating indicates an unexpectedly large decrease of the plasma frequency which is quite unusual in doped semiconductors. Note that a similar behavior has also been reported by Barker[15] and confirmed later[24] for oxygen-deficient strontium titanate.

Kozyreva[17] attempted to decouple the plasmon from the phonons but neglected damping. Our results show that coupling of the highest-frequency LO phonon with the plasmon increases the damping of the coupled mode by a factor as high as 12 at room temperature (Table I). A decoupling scheme which neglects damping introduces serious inaccuracies, especially in the frequency of the heavily damped plasmon. A simple way to decouple the system while including damping terms is to postulate a dielectric function which consists of two additive terms: a pure-phonon contribution of the form of Eq. (2) which

TABLE I. Frequency and damping coefficients (in cm^{-1} units) which yield the best fit to reflection spectra of a doped sample as shown in Fig. 2, compared with undoped strontium titanate.

$SrTiO_3$				$SrTiO_3$ (0.9% Nb)			
Transverse modes							
300 K		600 K		300 K		600 K	
Ω_{jTO}	γ_{jTO}	Ω_{jTO}	γ_{jTO}	Ω_{jTO}	γ_{jTO}	Ω_{jTO}	γ_{jTO}
89	27	128	34	100	48	132	45
175	5.5	179	16	175	10	181	18
544	18	538	35	550	19	540	34

Longitudinal modes											
				Decoupled modes				Coupled modes			
300 K		600 K		300 K		600 K		300 K		600 K	
Ω_{jLO}	γ_{jLO}	Ω_{jLO}	γ_{jLO}	Ω'_{jLO}	γ'_{jLO}	Ω'_{jLO}	γ'_{jLO}	Ω_{jLO}	γ_{jLO}	Ω_{jLO}	γ_{jLO}
172.5	3	173	9	171	5	176	10	171	5	176	10
475	5	472	9	471	11	469	12	505	38	479	32
796	26	790	46	796	27	789	45	924	340	817	190

	Plasmon	
	300 K	600 K
Ω_p	515	250
γ_p	390	210
γ_0	(40)	(40)

provides an excellent fit to the reflectivity of undoped $SrTiO_3$,[12] plus a plasmon contribution. The simplest expression for the plasmon contribution would be a Drude term

$$\varepsilon_{\rm pl}=-\varepsilon_\infty\Omega_p^2/[\omega(\omega-i\gamma_0)]\ , \tag{3}$$

but such a dielectric function model does not satisfactorily fit the present infrared data. Similar difficulties were encountered in reduced rutile[18] and more recently in copper-based high-T_c oxide superconductors.[2] As already discussed in Refs. 18, 19, and 23, Eq. (2) can provide a better fit to a plasmon mode alone under the form

$$\varepsilon=\varepsilon_\infty(\Omega_p^2-\omega^2+i\gamma_p\omega)/(-\omega^2+i\gamma_0\omega)\ . \tag{4}$$

Equation (4) may be rewritten

$$\varepsilon=\varepsilon_\infty+\varepsilon_{\rm pl}\ , \tag{5}$$

where $\varepsilon_{\rm pl}$ is now

$$\varepsilon_{\rm pl}=-\varepsilon_\infty[\Omega_p^2+i(\gamma_p-\gamma_0)\omega]/[\omega(\omega-i\gamma_0)]\ . \tag{6}$$

Note that Eq. (6) reduces to the Drude form, Eq. (3), when $\gamma_p=\gamma_0$. We thus rewrite the complete dielectric function in the form

$$\varepsilon/\varepsilon_\infty=\prod_j(\Omega'^2_{j\rm LO}-\omega^2+i\gamma'_{j\rm LO}\omega)/(\Omega'^2_{j\rm TO}-\omega^2+i\gamma'_{j\rm TO}\omega) -[\Omega_p^2+i(\gamma_p-\gamma_0)\omega]/[\omega(\omega-i\gamma_0)]\ . \tag{7}$$

The $\Omega'_{j\rm LO}$'s in the first term of the right-hand side of Eq. (7) are no longer the zeros of the dielectric function, but are now decoupled LO-phonon frequencies. Equation (7) is also found to yield an excellent fit to reflectivity data, essentially indistinguishable from that with Eq. (2). Parameters for decoupled phonons and plasmon which provide the best fit to the data of Fig. 2 are also listed in Table I. After such a double fitting procedure (i) with Eq. (2) for the coupled modes and (ii) with Eq. (7) for decoupled LO excitations, the very instructive picture summarized in Figs. 4–6 emerges. Note that both fitting procedures yield the same TO phonon parameters. Furthermore, the decoupled LO phonon frequencies turn out to be little affected by doping. This indicates that our decoupling procedure seems to be physically sound. Note that lowest-frequency mode 1 is little affected by coupling whereas modes 2 and 3 are much more (compare coupled and uncoupled mode dampings in Table I).

A plasmon can be treated phenomenologically like a phonon with a TO frequency which is set to zero (because there is no restoring force constant for the plasma-type motion). This is the origin of the divergence of the imaginary part of the dielectric response when the frequency tends towards zero as is shown in Fig. 7. In the same figure, the next FE soft mode is well visible nearby. But one cannot have two consecutive maximum without a minimum in between. A LO mode necessarily corresponds to this minimum. This LO mode is highly damped because its damping is large (compared to its low frequency) since it is blocked between two semibroad TO modes.

Coupled and decoupled phonon and plasmon contribu-

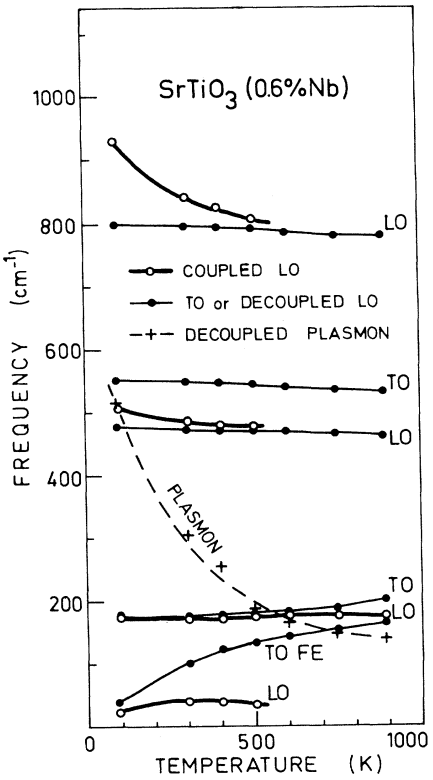

FIG. 4. Temperature dependence of coupled and decoupled excitations which yield a best fit to infrared reflection spectra.

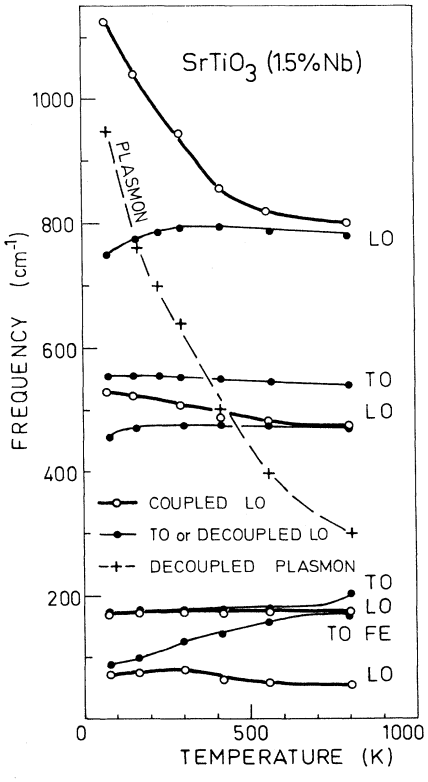

FIG. 5. Same legend as Fig. 4.

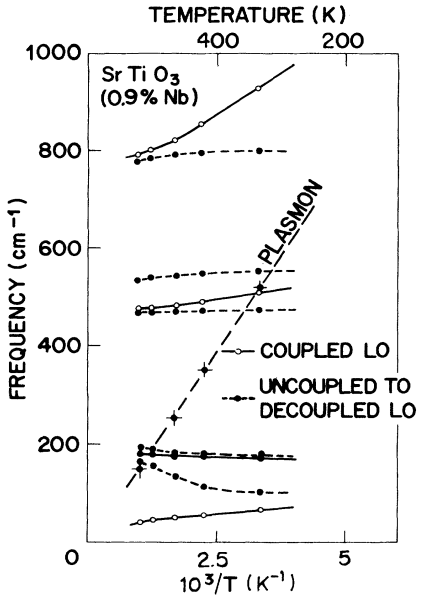

FIG. 6. Same legend as Fig. 4 (note inverted temperature scale).

tions to the imaginary part of the dielectric function and to the imaginary part of the inverse dielectric function are illustrated in Fig. 7. The frequency shift and increased damping of the longitudinal modes caused by coupling to the plasmon are visualized in Fig. 7.

III. RESULTS AND DISCUSSION

A. Soft ferroelectric mode

The TO soft FE mode would reach zero frequency at absolute zero temperature if quantum effects are ignored in undoped strontium titanate. Quantum effects stabilize the FE soft-mode frequency to a finite value at low temperatures, preventing the crystal from undergoing a transition to the ferroelectric state. The soft-mode frequency increases upon heating in such a sharp way that it would "cross" the next TO mode near 175 cm^{-1} above 1000 K if the coupling was ignored.[12] Actually, an energy level repulsion phenomenon occurs and causes a saturation of the low-frequency TO component and an upshift of the high-frequency TO mode. The same is found in doped samples as shown in Fig. 8. The upshift of the high-frequency TO coupled mode in the sample doped with 0.6% Nb is even more marked than in undoped $SrTiO_3$. A decoupling of the system with the aid of[25]

$$\Omega_{\pm}=1/2(\omega_{175}+\omega_{\text{soft}})\pm 1/2[(\omega_{175}-\omega_{\text{soft}})^2\pm 4w^2]^{1/2} \quad (8)$$

allows one to fit experimental TO data fairly well as shown in Fig. 8. The uncoupled TO nonsoft-mode frequency was assumed to be temperature independent at 175 cm^{-1}, and the coupling parameter is found to amount to $w=16$ cm^{-1}. A transfer of oscillator strength and damping rate between both TO excitations occurs at the highest investigated temperature. Results in doped and undoped samples are compared in Table II. TO oscillator strengths listed in this table are deduced from the TO-LO splittings via the relationship[19]

$$\Delta\varepsilon_j/\varepsilon_\infty=\Omega_{j\text{TO}}^{-2}\prod_k(\Omega_{k\text{LO}}^2-\Omega_{j\text{TO}}^2)\Big/\prod_{k\neq j}(\Omega_{k\text{TO}}^2-\Omega_{j\text{TO}}^2)\,. \quad (9)$$

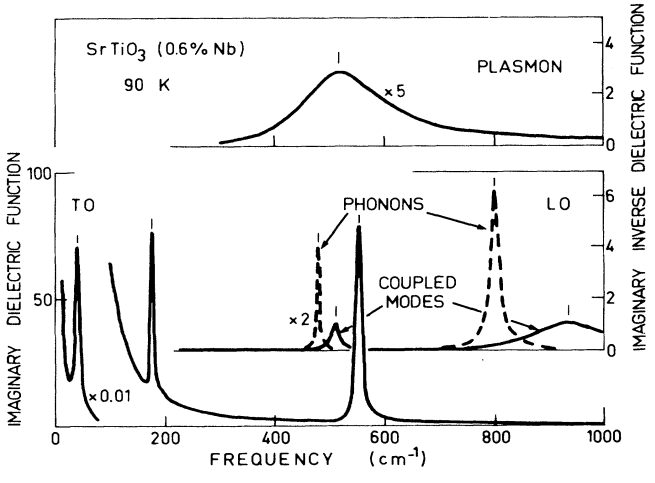

FIG. 7. Decoupling pattern of both lowest TO modes. Dashed straight lines represent decoupled TO modes. Dots are experimental data and solid heavy curves are the best fit of Eq. (8) to the data. Light solid lines represent uncoupled TO modes in undoped strontium titanate for comparison.

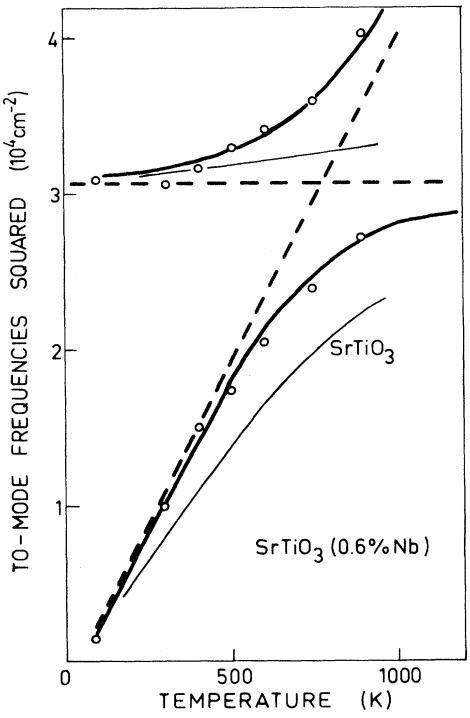

FIG. 8. Temperature and concentration dependence of the soft ferroelectric mode. Present data are compared with similar results obtained by neutron spectroscopy in reduced strontium titanate.

TABLE II. Low-frequency coupled TO mode parameters at 890 K in undoped strontium titanate compared with a sample doped with 0.6% Nb. Mode anticrossing which is achieved at this temperature manifests itself by a transfer of damping and oscillator strength.

		Ω_j (cm^{-1})	γ_j (cm^{-1})	$\Delta\varepsilon_j$
Undoped	TO^-	149	43	85
	TO^+	182	27	14
Doped	TO^-	165	28	26
	TO^+	201	80	38

Such a decoupling procedure has been performed in the three samples and the results for the temperature dependence of the decoupled soft FE mode frequency squared are summarized in Fig. 9. Soft-mode frequencies are found to shift up with doping. Solid and dashed lines represent our data. Symbols in Fig. 9 reproduce data obtained by inelastic-neutron-scattering experiments in reduced strontium titanate by Baüerle *et al.*[16] Behaviors observed in niobium-doped and oxygen-deficient samples are found to be very similar. Both treatments tend to stabilize the soft FE mode and to minimize the tendency of the crystal to reach a ferroelectric state as discussed in detail in Ref. 11.

B. Plasma response

The dielectric function of a crystal can be evaluated from the infrared reflectivity via a KK analysis when data are available over a frequency range wide enough. If we assume that this criterion is obeyed here and since we have already evaluated the parameters which describe the pure-phonon reflectivity with a fairly good accuracy, the plasma contribution to the dielectric function can be deduced from the experiment. We have restricted this additional analysis to those spectra where the plasmon contribution to the reflectivity is large enough. This has been achieved in the following way. We start from the representation

$$\varepsilon_{\rm pl}(\omega)=-\varepsilon_\infty\Omega_p^2(\omega)/\{\omega[\omega-i\gamma(\omega)]\}\ . \tag{10}$$

Here the plasma damping function is

$$\gamma(\omega)=\omega\varepsilon''_{\rm pl}/\varepsilon'_{\rm pl}\ . \tag{11}$$

We determine the functions $\Omega_p(\omega)$ and $\gamma(\omega)$ from the equality

$$\varepsilon_{\rm pl}(\omega)=\varepsilon_{\rm KK}(\omega)-\varepsilon_\infty\prod_j(\Omega'^2_{j\rm LO}-\omega^2+i\gamma_{j\rm LO}\omega)/(\Omega'^2_{j\rm TO}-\omega^2+i\gamma_{j\rm TO}\omega)\ , \tag{12}$$

where $\varepsilon_{\rm KK}(\omega)$ is deduced from a KK analysis of the experimental spectrum. Figure 10 shows the results of such a calculation for the sample with 0.9% Nb at the lowest temperature investigated, i.e., when the plasma frequency is the highest. The function is plotted only in the regions where the contribution of phonons is not too large. This calculation is just made to give an idea of the deviation

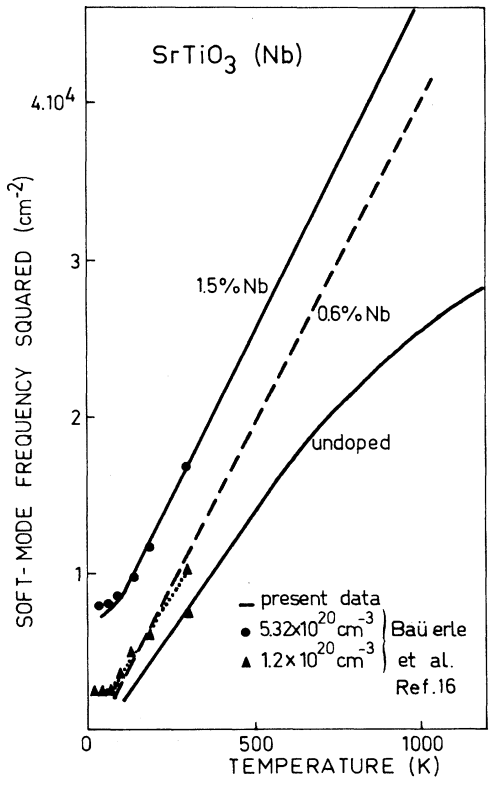

FIG. 9. Spectral response of coupled modes compared to decoupled phonons and plasmon.

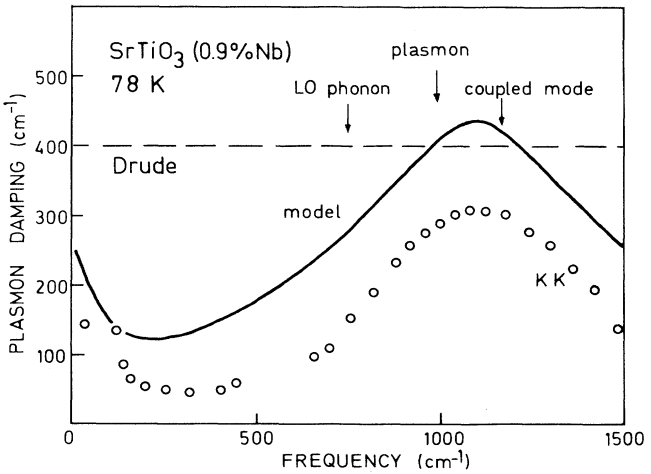

FIG. 10. Plasmon damping function deduced from a Kramers-Kronig analysis, compared with the model memory function equation (15) used to improve the fit to the infrared reflection spectrum shown in Fig. 11.

from the experimental data with respect to the oversimplified Drude profile in the extreme cases. It is clear from our result why a Drude term with a constant damping cannot fit such data satisfactorily. The fact that Barker[15] fitted his data with a Drude term is not significant (i) because the agreement with experiment was generally poorer than in Figs. 2 and 3, and (ii) because no data were available below 350 cm^{-1}, thus making it impossible to check the validity of the model in the whole relevant spectral range.

Coming back to the factorized form of the dielectric function used in Sec. II, and comparing Eqs. (6) and (10), one gets

$$\Omega_p^2/\{\omega[\omega-i\gamma(\omega)]\}=[\Omega_p^2+i(\gamma_p-\gamma_0)\omega]/[\omega(\omega-i\gamma_0)] \tag{13}$$

and, neglecting terms of order γ^2,

$$\gamma(\omega)=\gamma_0+(\gamma_p-\gamma_0)\omega^2/\Omega_p^2 \ . \tag{14}$$

Consequently, our previous ansatz equation (6) makes a specific assumption about the form of the plasmon damping function which varies monotonically according to (14) from γ_0 at $\omega=0$ up to γ_p at $\omega=\Omega_p$. The model equation (6) thus roughly approximates the actual damping function but its tendency to increase with frequency is properly taken into account. This is the reason why a fairly good fit can be achieved with this model. A similar discussion referring to the assumptions of the model equation (2) about the phonon self-energy was developed in Ref. 19.

Barker[15] reported an additional feature in the reflectivity near 2000 cm^{-1}. This feature is also visible in Ref. 17. He assigned this feature to a polaron absorption and indicated that an additional Gaussian mode yields the best fit to this feature. An unusual dispersion is also observed in the range 1000–3000 cm^{-1} in our spectra of the unannealed samples. However, this feature practically ceases to be observable after annealing above 900 K. Notice, however, that Eq. (7) fits the reflectivity of the room-temperature spectrum of the sample with 0.9% Nb unsatisfactorily just between 1000 and 3000 cm^{-1} as seen in Fig. 2. This may indicate that an additional contribution may be present, although weak. Since its "intensity" seems to vary as the plasma damping level (the parameter that annealing controls mainly), it could be a structure in the damping function rather than an additional mode with a finite oscillator strength. There is an additional and more natural reason for testing a plasmon damping function. Infrared reflectivity spectra obtained at low temperatures in the case of both most heavily doped samples cannot be fitted perfectly with the model equation (7). Figure 10 indicates a broad peak roughly centered at the frequency of the highest LO phonon-plasmon-coupled mode plus another weaker one at zero frequency. To account for this situation phenomenologically, we have simply used a memory function[26]

$$M_m(\omega)=\gamma_m\Gamma_m/(\Omega_L-\omega+i\Gamma_m) \ , \tag{15}$$

which is introduced in the general representation

$$\varepsilon_{pl}(\omega)=-\varepsilon_\infty\Omega_p^2/\{\omega[\omega-M(\omega)]\} \ . \tag{16}$$

An example of the best fit achieved with this model is shown in Fig. 11 and compared to a simple Drude term where $M(\omega)$ reduces to a constant $-i\gamma_0$. The frequency dependence of the model damping function in that case is also shown in Fig. 10. Of course, there could be other ways to account for the discrepancies in the limiting case discussed here, and one should not attach excessive weight to the fact that this model works well.

C. Temperature dependence of plasma frequency

The dependence of the plasma frequency on temperature is plotted in Figs. 4–6 to visualize the mode-coupling pattern. Plasmon frequencies are reproduced in a summary plot in Fig. 12. Figure 6 shows a linear dependence upon the inverse temperature. Thus, in the four compounds, the plasma frequency is found to decrease by a factor of 4–6 when the temperature is increased from liquid nitrogen up to 1000 K. This behavior is very unusual. It implies not only that the system is degenerate but also, as found by Frederikse, Thurber, and Hosler[27] and discussed by Barker,[15] that the effective mass of charge carriers increases sharply upon heating. In our samples, Ω_p increases by 70, 90, and 50% upon cooling from 300 K down to 78 K in the samples doped with 0.6, 0.9, and 1.5 % of niobium, respectively. The average ratio 1.7 agrees fairly well with the square root of the experimental ratio 1.6 of electron effective masses deduced from the electronic specific heat and thermoelectric power, viz., $6m_e$ at 78 K and $16m_e$ at room temperature.[28] This is a straightforward application of the relation

$$\Omega_p^2=4\pi ne^2/m_e^*\varepsilon_\infty \ . \tag{17}$$

The m_e values given above concern a sample with a carrier concentration $n=1.4\times10^{20}$ cm^{-3}. The agreement means that the possible temperature dependence of n may be ignored in a first approximation, but no definite conclusion can be drawn in the absence of similar transport measurements in the samples we have studied. Eagles[28] proposed a model that attempts to explain the electronic properties of strontium titanate by a mixture of small and large polarons. In that case, since the proportion of the type of polarons with the larger mass increases as the energy of the polaron increases, thus increasing the average

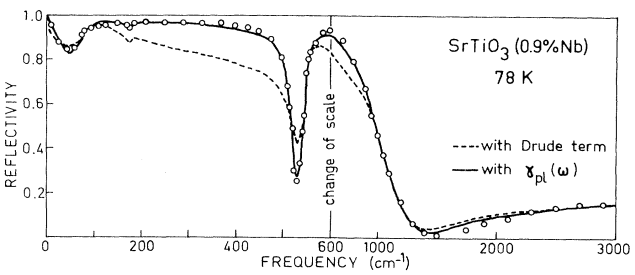

FIG. 11. A comparison of a best fit with a simple Drude term and with the plasmon damping function shown in Fig. 10.

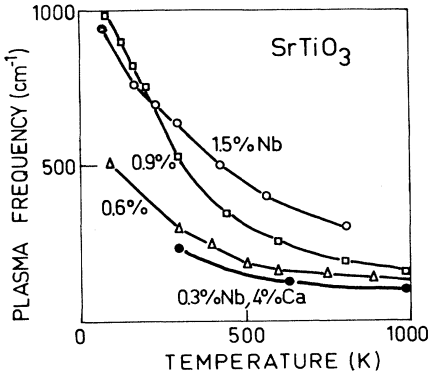

FIG. 12. Temperature and concentration dependence of the plasma frequency.

mass with temperature, Eagles calculated the increase of the density-of-states mass. He found $6m_e$, $6.5m_e$, and $22m_e$ at 0, 78, and 300 K, respectively. While the values fit the experiment at low temperature, the discrepancy at room temperature reaches 40% but the sign of variation is correct. On the other hand, the assumptions of small polarons in strontium titanate used by Eagles[28] is contradictory with the interpretation of transport measurements[27] which rather support a band, i.e., large polaron, picture. Other reasons could account for a variation of the effective mass. Fundamental absorption edge measurements in undoped strontium titanate reported by Goldschmit and Schuller[29] were understood in terms of a crossover from an indirect band gap below 500 K to direct band gap above 700 K. And one may wonder whether this specific situation would not contribute to the very unusual behavior observed here.

In summary, we have reported a complete study of infrared reflection spectra of niobium-doped n-type strontium titanate. From the point of view of the ferroelectric soft-mode behavior and the very unusual temperature dependence of the plasma frequency, our results confirm previous observations reported for oxygen-deficient strontium titanate in a narrower temperature range, and extend them. Results are consistent with transport measurements indicating a temperature dependence of the effective mass. It is not clear whether these results are related to the specific band scheme of strontium titanate or if they open the way to a more general view, and have to be kept in mind to analyze some surprising infrared properties of high-T_c oxide superconductors in the normal state. Further investigations are highly desirable.

[1]J. G. Bednorz and K. A. Müller, Z. Phys. B **64**, 189 (1986).
[2]T. Timusk and D. B. Tanner, in *Physical Properties of High-Temperature Superconductors,* edited by M. Ginsberg (World Scientific, Singapore, 1989), Vol. 1, p. 341.
[3]F. F. Schooley, W. R. Hosler, and M. L. Cohen, Phys. Rev. Lett. **12**, 474 (1964).
[4]C. S. Koonce, M. L. Cohen, J. F. Scooley, W. R. Mosler, and E. R. Pfeiffer, Phys. Rev. **163**, 380 (1969); J. Appel, *ibid.* **180**, 508 (1969); K. L. Ngai, Phys. Rev. Lett. **32**, 215 (1974); Y. Takada, J. Phys. Soc. Jpn. **49**, 1267 (1980).
[5]A. W. Sleight, J. L. Gilson, and P. E. Biersted, Solid State Commun. **17**, 27 (1975).
[6]L. F. Mattheis and D. R. Hamann, Phys. Rev. Lett. **60**, 2681 (1988).
[7]M. Licheron and F. Gervais, Mater. Sci. Eng. B **15**, L1 (1992).
[8]M. Licheron and F. Gervais, Phys. Rev. B **47**, 8008 (1993).
[9]F. Gervais and W. Kress, Phys. Rev. B **11**, 4809 (1985).
[10]R. Migoni, H. Bilz, and D. Baüerle, Phys. Rev. Lett. **37**, 1155 (1976).
[11]A. Bussman, H. Bilz, R. Roenspiess, and K. Schwarz, Ferroelectrics **25**, 343 (1980); H. Bilz, A. Bussman, G. Benedeck, H. Büttner, and D. Strauch, *ibid.* **25**, 339 (1980); A. Bussman-Holder, H. Bilz, D. Baüerle, and D. Wagner, Z. Phys. B **41**, 353 (1981).
[12]J. L. Servoin, Y. Luspin, and F. Gervais, Phys. Rev. B **22**, 5501 (1980).
[13]D. Rytz, M. D. Fontana, J. L. Servoin, and F. Gervais, Phys. Rev. B **28**, 6041 (1983).
[14]F. Gervais, Jpn. J. Appl. Phys. Suppl. **24-2**, 198 (1985).
[15]A. S. Barker, in *Optical Properties and Electronic Structure of Metals and Alloys,* edited by F. Abeles (North-Holland, Amsterdam, 1976), p. 453.
[16]D. Wagner, D. Baüerle, F. Schwabl, B. Dorner, and H. Kraxemberger, Z. Phys. B **37**, 317 (1980); D. Baüerle, D. Wagner, M. Wötleche, B. Dorner, and H. Kraxemberger, *ibid.* **38**, 335 (1980).
[17]M. S. Kozyreva, Opt. Spectrosc. **43**, 51 (1977).
[18]J. F. Baumard and F. Gervais, Phys. Rev. B **15**, 2316 (1977).
[19]F. Gervais, in *Infrared and Millimeter Waves,* edited by K. J. Button (Academic, New York, 1983), Vol. 8, p. 279.
[20]W. G. Spitzer, R. C. Miller, D. A. Kleinman, and L. E. Howarth, Phys. Rev. **126**, 1710 (1962).
[21]A. S. Barker and J. J. Hopfield, Phys. Rev. **135**, A1732 (1964).
[22]D. A. Ledsham, W. G. Chambers, and T. J. Parker, Infrared Phys. **17**, 165 (1977).
[23]F. Gervais and J. F. Baumard, Solid State Commun. **21**, 861 (1977).
[24]F. Gervais, P. Echegut, J. M. Bassat, and P. Odier, Phys. Rev. B **37**, 9364 (1988).
[25]J. F. Scott, Rev. Mod. Phys. **46**, 83 (1974).
[26]W. Götze and P. Wölfe, Phys. Rev. B **6**, 1226 (1972).
[27]H. P. R. Frederikse, W. R. Thurber, and W. R. Hosler, Phys. Rev. **134**, A442 (1964).
[28]D. M. Eagles, in *Physics of Disordered Materials,* edited by D. Adler (Plenum, New York, 1985), p. 357.
[29]D. Goldschmidt and H. L. Tuller, Phys. Rev. B **35**, 4360 (1987).